Spectral characterization of Dictyostelium autofluorescence

Engel, R.; van Haastert, P. J. M.; Visser, Antonie J.W.G.

Published in:
Microscopy Research and Technique

DOI:
10.1002/jemt.20282

Spectral Characterization of *Dictyostelium* Autofluorescence

RUCHIRA ENGEL,[1] PETER J.M. VAN HAASTERT,[2] AND ANTONIE J.W.G. VISSER[1]*
[1]*MicroSpectroscopy Centre, Laboratory of Biochemistry, Wageningen University, 6703 HA Wageningen, The Netherlands*
[2]*Department of Biochemistry, University of Groningen, 9747 AG Groningen, The Netherlands*

KEY WORDS spectral imaging; fluorescence fluctuation spectroscopy; confocal microscopy; chemotaxis

ABSTRACT *Dictyostelium discoideum* is used extensively as a model organism for the study of chemotaxis. In recent years, an increasing number of studies of *Dictyostelium* chemotaxis have made use of fluorescence-based techniques. One of the major factors that can interfere with the application of these techniques in cells is the cellular autofluorescence. In this study, the spectral properties of *Dictyostelium* autofluorescence have been characterized using fluorescence microscopy. Whole cell autofluorescence spectra obtained using spectral imaging microscopy show that *Dictyostelium* autofluorescence covers a wavelength range from ~500 to 650 nm with a maximum at ~510 nm, and thus, potentially interferes with measurements of green fluorescent protein (GFP) fusion proteins with fluorescence microscopy techniques. Further characterization of the spatial distribution, intensity, and brightness of the autofluorescence was performed with fluorescence confocal microscopy and fluorescence fluctuation spectroscopy (FFS). The autofluorescence in both chemotaxing and nonchemotaxing cells is localized in discrete areas. The high intensity seen in cells incubated in the growth medium HG5 reduces by around 50% when incubated in buffer, and can be further reduced by around 85% by photobleaching cells for 5–7 s. The average intensity and spatial distribution of the autofluorescence do not change with long incubations in the buffer. The cellular autofluorescence has a seven times lower molecular brightness than eGFP. The influence of autofluorescence in FFS measurements can be minimized by incubating cells in buffer during the measurements, prebleaching, and making use of low excitation intensities. The results obtained in this study thus offer guidelines to the design of future fluorescence studies of *Dictyostelium*. *Microsc. Res. Tech. 69:168–174, 2006.*

INTRODUCTION

Dictyostelium discoideum is used extensively as a model organism for the study of chemotaxis, the process of cell movement along a chemical gradient, because of its resemblance to mammalian cell movement. As a model system *Dictyostelium* offers many advantages, which include its genetic manageability and easy access for biochemical and biological studies. In recent years, the chemotaxis mechanism of *Dictyostelium* has been increasingly probed using fluorescence-based techniques. The phenomenon of fluorescence, by virtue of its multiple characteristics—intensity, brightness, lifetime, excitation-emission spectra, resonance energy transfer, to name a few—can be exploited to specifically study the behavior of one type of molecules in a medley of diverse molecules in the cell. The possibility of fusing the protein of interest to intrinsically fluorescent proteins, such as the green fluorescent protein (GFP), without loss of its normal function and localization (Tsien, 1998), has made fluorescence-based techniques a powerful tool available to biologists today to study various processes in living cells.

Fluorescence microscopic and spectroscopic techniques applied to study *Dictyostelium* chemotaxis include the use of confocal imaging to study localization and dynamics of cellular proteins e.g., G-proteins (Blaauw et al., 2003; Jin et al., 2000), pleckstrin homology domain of the cytosolic regulator of adenylyl cyclase (Parent et al., 1998), adenylyl cyclase A (Kriebel et al., 2003), guanylyl cyclase (Veltman et al., 2005), actin cytoskeleton (Fischer et al., 2004; Uchida and Yumura, 2004); the use of fluorescence recovery after photobleaching to study cellular viscosities and diffusion of actin or actin-binding proteins (Bretschneider et al., 2002; Potma et al., 2001) and the use of Förster resonance energy transfer to detect interaction between G-protein subunits (Janetopoulos et al., 2001; Xu et al., 2005). In addition, fluorescence fluctuation spectroscopy (FFS) has been used to study the diffusion of GFP-tagged proteins in *Dictyostelium* cells (Ruchira et al., 2004). FFS, comprising techniques such as fluorescence correlation spectroscopy (FCS) and photon counting histogram (PCH) analysis, makes use of tiny, spontaneous fluorescence intensity fluctuations in a small volume (<1 fL (femtolitre)) to extract information about their physical parameters (Haustein and Schwille, 2003; Hess et al., 2002; Levin and Carson, 2004; Vukojevic et al., 2005). Because of its high sensitivity, FFS can be used for detection at the single molecule level and can thus provide a means to study the behavior of biomolecules in cells at physiologically relevant concentrations.

*Correspondence to: Antonie J.W.G. Visser, MicroSpectroscopy Centre, Laboratory of Biochemistry, Wageningen University, Dreijenlaan 3, 6703 HA Wageningen, The Netherlands. E-mail: ton.visser@wur.nl

Received 26 June 2005; accepted in revised form 15 September 2005
DOI 10.1002/jemt.20282
Published online in Wiley InterScience (www.interscience.wiley.com).

Intrinsic cellular fluorescence is one of the major factors that can interfere with the application of fluorescence-based techniques in cells. Autofluorescence caused by endogenous molecules such as flavins, flavoproteins, and NAD(P)H (Aubin, 1979; Benson et al., 1979) can bias a measurement and reduce the signal to noise ratio (SNR). Thus, knowledge of autofluorescence characteristics is essential to avoid or minimize its influence. In the present study, we have characterized the spectral properties of *Dictyostelium* autofluorescence using fluorescence spectral imaging microscopy (FSPIM). The spatial distribution of autofluorescence and its intensity at different excitation wavelengths has been visualized using confocal laser scanning microscopy (CLSM). FFS was used to quantify molecular brightness and intensity in cells under different experimental conditions. The results obtained in this study offer guidelines to the design of future fluorescence studies of *Dictyostelium*.

MATERIALS AND METHODS

Sample Preparation

Wild type *Dictyostelium discoideum* of strain AX3 were grown in HG5 medium that was composed of 14.3 g/L peptone, 7.15 g/L yeast extract, 0.54 g/L Na_2HPO_4, 0.49 g/L KH_2PO_4, and 10.0 g/L glucose. Cells were withdrawn from a confluent petriplate and were either directly used or washed twice in potassium phosphate buffer (pH 6.5, 17 mM) before use. For FSPIM measurements, cells were placed on a microscope slide (Menzel-Glaser, Germany) and allowed to settle, after which a coverglass was gently placed on top. For confocal imaging and FFS measurements, cells were transferred to a 96-chambered glass-bottom microplate (Whatman, USA). Cells were starved by suspending vegetative cells at a density of 2.5×10^7 ml^{-1} in 500 μL of potassium phosphate buffer in a 15-mL centrifuge tube (Sarstedt, The Netherlands) for ~5 h. After 5 h, small cell aggregates could be observed. FSPIM spectra were also obtained from 200 nM eGFP (F64L, S65T) dissolved in 50 mM Tris buffer (pH 8) and from 100 μM flavin mononucleotide (FMN) (Sigma, The Netherlands) dissolved in demineralised water.

Fluorescence Microscopy

Fluorescence Spectral Imaging Microscopy. The fluorescence spectra were obtained on a FSPIM setup comprising a Leica DMR epifluorescence microscope equipped with a 250IS imaging spectrograph (Chromex) coupled to a CH250 CCD camera (Photometrics, The Netherlands) (Hink et al., 2003). A 100-W mercury arc lamp provided the excitation light, which was filtered using a 435 DF 10 bandpass filter (Omega) and a 470DRLP dichroic mirror (Omega, The Netherlands). Fluorescence spectral images were acquired with the FSPIM setup using a Leica Plan Neofluar 40× oil immersion (NA 1.0) objective and a 475 longpass emission filter (Schott, Germany) using an integration time of either 10 or 15 s. The emission spectra were recorded from 475 to 725 nm and corrected for background fluorescence and camera bias by subtracting an extracellular region from the same spectral image. The spectra for HG5, eGFP, and FMN were corrected by subtracting a spectral image of water.

Confocal Laser Scanning Microscopy. Confocal images of cells were obtained with a confocal laser-scanning microscope (ConfoCor 2–LSM 510 combination setup, Carl-Zeiss, Germany), which is described in detail elsewhere (Hink et al., 2003). Autofluorescence was excited with 458 and 488 nm wavelengths from an argon-ion laser and with 633 nm wavelength from a He-Ne laser, focused into the sample by a C-Apochromat 40× water-immersion objective with NA 1.2 (Zeiss). The excitation power during image acquisition was ~30 μW for the 458-nm laser line and 200 μW for the 488- and 633-nm laser lines. The fluorescence was passed through the main beam splitters HFT 458, 488, and 514/633 and was filtered using longpass filters 475, 505, and 650. Differential interference contrast (DIC) images were also acquired simultaneously. The acquired images were processed using Zeiss LSM Image Browser software package (V 3.2).

Fluorescence Fluctuation Spectroscopy. FCS and PCH measurements were performed with Zeiss-Evotec ConfoCor, as has been described previously (Ruchira et al., 2004). Autofluorescent molecules were excited with a wavelength of 488 nm from an argon-ion laser, the power of which was attenuated with neutral-density filters. For the quantification of autofluorescence of cells under different conditions, and for PCH analysis, measurements were performed at a power of ~10 μW. Measurement duration in all cases was 10 s. In order to photobleach the autofluorescent molecules, cells were exposed to ~1 mW laser power, for the times mentioned. For PCH analysis, between 3×10^5 and 1×10^6 photons were collected and the data were analyzed at a sampling frequency of 20 kHz. The autofluorescence characteristics of vegetative cells incubated in buffer were measured at excitation intensities of 3, 10, 20, 70, 200, and 670 μW.

The FCS data were analyzed using the FCS data processor software package V 1.4 (Skakun et al., 2005). The data were fit to a model describing the Brownian motion of molecules in three dimensions, given in Eq. (1).

$$G(\tau) = 1 + \frac{1}{N}\sum_i \phi_i \frac{1}{\left(1+\frac{\tau}{\tau_{di}}\right)\sqrt{1+\left(\frac{\omega_{xy}}{\omega_z}\right)^2\frac{\tau}{\tau_{di}}}} + \text{offset} \quad (1)$$

$$\text{where, } \phi_i = \frac{\epsilon_i^2 Y_i}{\left(\sum_i \epsilon_i Y_i\right)^2} \quad (2)$$

In Eq. (1), $G(\tau)$ is the autocorrelation function, N is the average number of molecules in the 3D Gaussian volume of radial radius ω_{xy} and axial radius ω_z. The molecules of species i have a diffusion time $\tau_{d,i}$, molecular brightness ϵ_i and molar fraction Y_i. If only one species is present, ϕ_i becomes 1. The offset term in the equation accounts for slow drifts in the intensity fluctuation trace (in the time scales of seconds) due to which the autocorrelation function does not decay to 1 at infinitely long times (Brock et al., 1999).τ_d is related to the translational diffusion coefficient D as:

$$\tau_d = \frac{\omega_{xy}^2}{4D} \quad (3)$$

The 3D Gaussian volume is given as (Schwille et al., 1997):

$$V_{3DG} = \pi^{3/2}\omega_{xy}^2\omega_z \quad (4)$$

The average concentration of the fluorescent species in the sample can be calculated using N and V_{3DG}.

$$C = \frac{N}{V_{3DG}A} \quad (5)$$

In Eq. (5), A is the Avogadro's number, which is 6.023×10^{23}. The instrument was calibrated with the dye rhodamine-110 (Molecular Probes, The Netherlands) ($D = 2.8 \times 10^{-10}$ m^2/s), which gave a value of 10 for the ratio ω_z/ω_{xy}, also called the structural parameter, and $\tau_d = 55$ μs. V_{3DG} was calculated to be 0.85 fL. The D values for autofluorescent molecules could be subsequently calculated from the obtained τ_d and using Eq. (3).

The PCH data were fit assuming single species. The PCH function for an open detection volume describes the possibility of observing k photon counts per sampling time with N as the average number of molecules in the detection volume (Chen et al., 1999). The molecular brightness ϵ, expressed as kHz/molecule, is the ratio of the average number of photon counts $\langle k \rangle$ received per second to N (Eq. (6)). ϵ is independent of the sampling frequency and as a result values from different experiments can be directly compared (Chen et al., 1999).

$$\epsilon = \frac{\langle k \rangle}{N} \quad (6)$$

RESULTS

Autofluorescence Spectrum

Average autofluorescence spectra from wild-type *Dictyostelium* cells of strain AX3 were acquired using FSPIM (Fig. 1). The autofluorescence spectrum is broad and asymmetric with a peak at 510 nm and a slight shoulder around 565 nm. For comparison, emission spectra of eGFP, of the growth medium HG5, and of FMN, an enzymatic cofactor thought to be a constituent of cellular autofluorescence (Aubin, 1979; Benson et al., 1979), were obtained under similar experimental conditions (Fig. 1).

The autofluorescence spectrum covers the entire region (475–625 nm) in which GFP also emits. The maximum in the autofluorescence spectrum is very close to the eGFP emission maximum (~508 nm), indicating that it can potentially interfere with measurements of GFP-fusion proteins. The HG5 medium, taken up by cells as they grow in it, is also fluorescent and displays a broad but characteristic spectrum. The spectrum, which is broader than the autofluorescence spectrum, also exhibits a peak around 510 nm and a slight shoulder around 565 nm. The ratio of the shoulder to the emission maxima, however, is different from the autofluorescence spectrum. The growth medium, which consists of yeast extracts containing vitamin B_2 (riboflavin), has previously been suggested as the reason for *Dictyostelium* autofluorescence (http://dictybase.org/techniques/lowflomedium.htm). The free FMN spectrum was however, slightly red-shifted with a peak at 525 nm and no shoulder. Since the fluorescence of flavin nucleotides is sensitive to its environment, it is very likely that in the growth medium and in the cells, where the nucleotides may be present in association with proteins or peptides, the fluorescence spectrum is affected (Aubin, 1979; Benson et al., 1979; Visser et al., 2001).

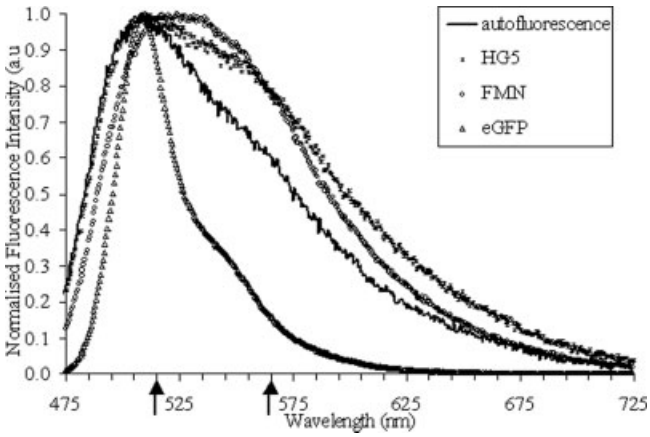

Fig. 1. Autofluorescence spectrum. A comparison of the average *Dictyostelium* autofluorescence spectrum, calculated from 10 cells incubated in potassium phosphate buffer (17 mM, pH 6.5), to the spectra of HG5, eGFP in Tris buffer (50 mM, pH 8), and FMN in water. Excitation wavelength is 435 nm. The arrows on the *x*-axis denote the transmission range of the bandpass emission filter 515–565, used in the FFS measurements. The spectra are normalized to the maximum intensity.

Visualizing Autofluorescence With Confocal Microscopy

The whole cell FSPIM spectrum gives important information about the emission characteristics of the autofluorescent molecules. The spatial distribution of the autofluorescence at different excitation wavelengths was then visualized using CLSM. Figure 2 shows the images acquired with excitation wavelengths of 458, 488, and 633 nm. The images show a patchy autofluorescence pattern that does not change when cells start aggregating. The images acquired at 633 nm excitation (Fig. 2C) show no detectable fluorescence signal, indicating that the interference of autofluorescence can be minimized by the use of fluorophores that can be excited in this region. Cells incubated in the growth medium (Fig. 3A) exhibit higher autofluorescence than cells incubated in buffer (Fig. 3B), indicating that the fluorescent growth medium taken up by the cells contributes to the autofluorescence. To investigate if the autofluorescence intensity decreased as cells exchanged the fluorescent medium for the nonfluorescent buffer, a series of images of cells incubated in buffer for various times was made. The autofluorescence intensity of cells incubated in buffer for 2 h is similar to the intensity of cells incubated in buffer for 20 min (Fig. 3). Thus, it appears that the exchange of medium for buffer takes place within the first 20 min and thereafter the average autofluorescence intensity does not change perceptibly. This fast exchange rate is in accordance with previous studies on fluid uptake by *Dictyostelium* cells grown in liquid

medium (Aguado-Velasco and Bretscher, 1999; Kayman and Clarke, 1983). AX3 cells have a fluid uptake rate of ~4 fL/cell/min (Kayman and Clarke, 1983). Approximating the cell to a hemisphere of 5 μm radius, the cell volume is ~250 fl, which means that in 20 min a cell can exchange fluid equivalent to one-third of its total volume. Since autofluorescence appears to cover ~20% of the cell volume (Figs. 2 and 3), this means that in 20 min the cells can effectively get rid of any fluorescence due to the growth medium.

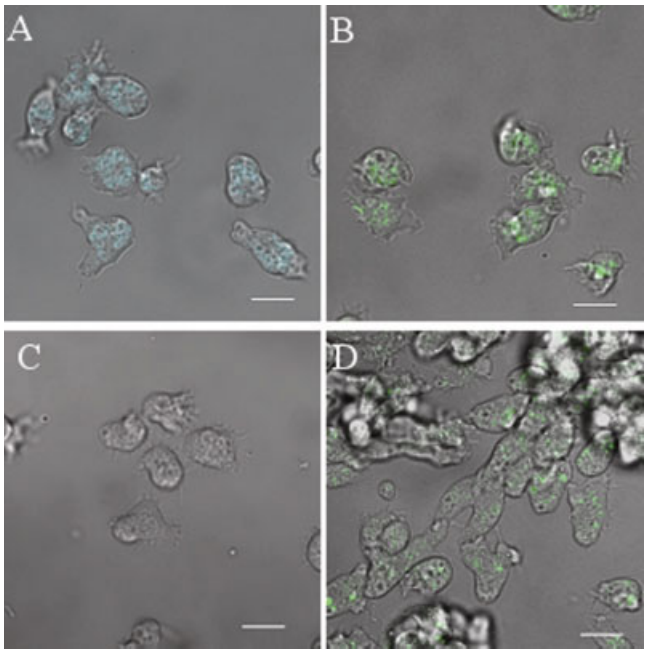

Fig. 2. *Dictyostelium* autofluorescence imaged with fluorescence confocal laser scanning microscope. Vegetative AX3 cells incubated in buffer were excited at (**A**) 458 nm (**B**) 488 nm, and (**C**) 633 nm wavelength. Fluorescence was filtered using longpass filters 475, 505, and 650. Aggregating cells (**D**) were excited at 488 nm. Images shown are merge of DIC and fluorescence images. Bar = 10 μm.

Fluorescence Fluctuation Spectroscopy of Autofluorescent Molecules

Further characterization of the autofluorescence intensity and molecular brightness was performed with FCS and PCH analysis. Autofluorescent molecules were excited with the 488 nm wavelength, and fluctuation intensity traces and autocorrelation curves from cells under different experimental conditions were recorded. The autofluorescence intensity shows wide variation from cell to cell and the fluctuation intensity traces display large nonuniform fluctuations (Fig. 4). The average intensity obtained from a 10-s measurement in a cell was taken as the average autofluorescence intensity of that cell.

The autofluorescence dependence on laser power was first studied. AX3 cells incubated in buffer were excited with increasing power of the 488-nm laser line. With increasing laser powers the autofluorescence intensity initially increases linearly and then reaches saturation (Fig. 5). The autocorrelation curves recorded at the different laser powers are noisy, indicating low SNRs (Fig. 6). The curves were evaluated using Eq. (1). At excitation intensities of ~700 and 200 μW fast diffusion with average diffusion coefficient value of 220 ± 50 $\mu m^2/s$ ($n = 13$) is observed. The diffusion appears slower, with an average diffusion coefficient value corresponding to 47 ± 23 $\mu m^2/s$ ($n = 11$), when the excitation power is ~70 and 20 μW. Below excitation intensities of 20 μW, the curves became too noisy to be evaluated. The apparently fast diffusion at higher intensities can be due to intense photobleaching or other fast photophysical effects, e.g., triplet state dynamics and blinking, at these intensities (Widengren, 2001).

Since at excitation intensities below 20 μW the autofluorescence intensity fluctuations do not autocorrelate, it is more favorable to perform FCS measurements on GFP fusion proteins at these intensities. This

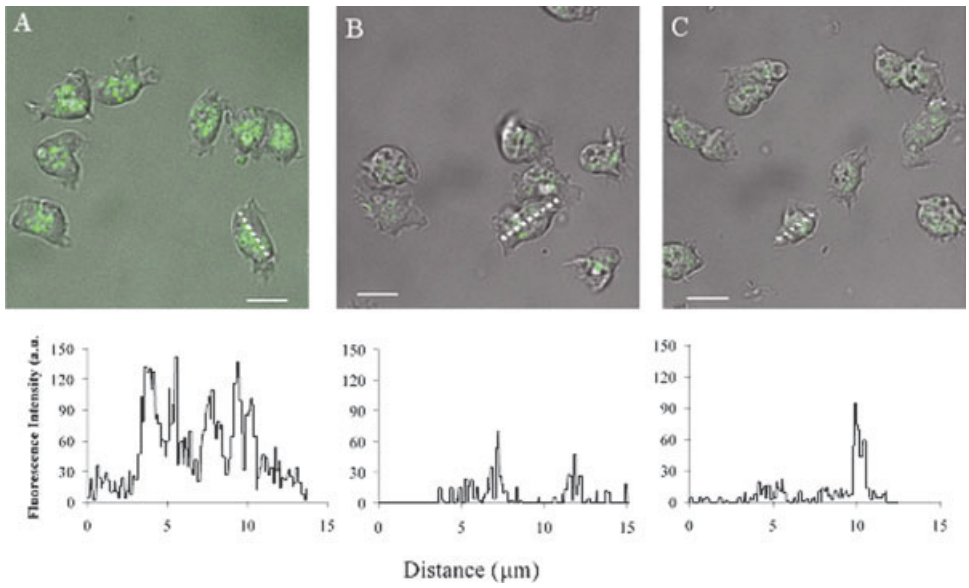

Fig. 3. Autofluorescence images of AX3 cells incubated in HG5 medium or buffer for different periods. **A:** Cells in HG5 medium, (**B**) in buffer for 20 min, and (**C**) in buffer for 2 h. The lower panels show the corresponding fluorescence intensity profiles taken along the white dotted line through a cell in each image. Excitation wavelength is 488 nm. Bar = 10 μm.

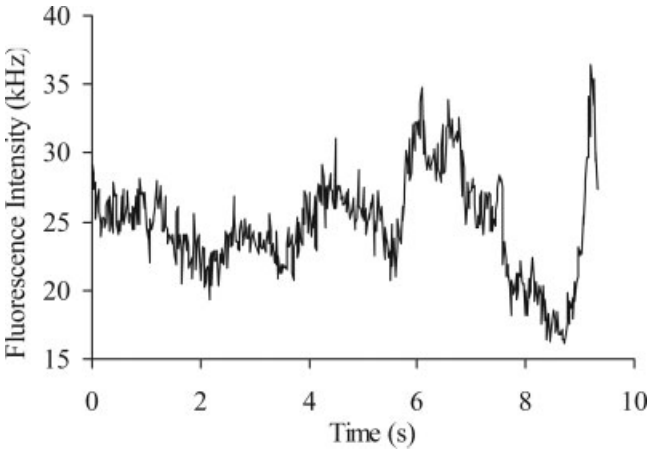

Fig. 4. Autofluorescence intensity fluctuation. Representative curve of the fluorescence intensity trace obtained from a single measurement in an AX3 cell incubated in potassium phosphate buffer (pH 6.5, 17 mM) and excited with ~10 μW power of the 488-nm laser line.

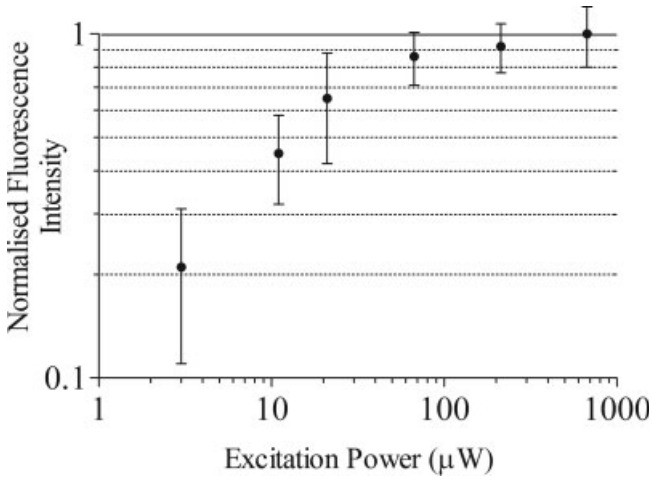

Fig. 5. Average autofluorescence intensity depends on the excitation power. Plot shows the normalized intensities obtained from *Dictyostelium* AX3 cells incubated in buffer excited with varying powers of the 488-nm laser.

would eliminate unwanted contribution of the autofluorescent species to the autocorrelation curve. The presence of noncorrelating background does not affect the diffusion times obtained from FCS curves. However, it does lower the amplitude of the correlation curve leading to an apparently higher number of molecules in the detection volume (Brock et al., 1998), which can be corrected for as described in Eq. (7)

$$N_{\text{corr}} = N_{\text{total}}\left(1 - \frac{F_{\text{background}}}{F_{\text{total}}}\right)^2 \qquad (7)$$

where N_{corr} and N_{total} are the average corrected and uncorrected number of molecules in the detection volume, $F_{\text{background}}$ is the autofluorescence intensity, and F_{total} is the total fluorescence intensity including background and GFP fluorescence. Tolerating a maximum error of 15% in determination of N_{corr}, the autofluorescence at excitation intensities below 20 μW can be ignored if F_{total} is at least 14 times higher than $F_{\text{background}}$.

The average autofluorescence intensities of cells excited at ~10 μW, under different experimental conditions, were next investigated (Table 1). Cells incubated in HG5 medium have the most intense autofluorescence signal (85 kHz), which reduces by 50% when the medium is replaced with buffer (44 kHz). In agreement with the confocal imaging this value does not change further with time. The autofluorescence can be photobleached by short exposure to the laser light. The autofluorescence of cells incubated in buffer reduces by 65% upon exposure to ~1 mW laser power for 1–2 s. Under similar experimental conditions, free GFP expressed in *Dictyostelium* cell cytoplasm shows ~45% decrease in its fluorescence intensity (data not shown). The slower photobleaching rate of GFP compared with the autofluorescent molecules indicates that the SNR in FFS measurements can be increased by photobleaching the autofluorescent molecules. Further reduction in autofluorescence intensity, up to 85% compared with initial values for cells incubated in buffer, can be obtained by exposing cells to 1 mW laser power for 5–7 s. During photobleaching, the microscope stage was moved so that the whole cell could be exposed to the high intensity beam. In this manner autofluorescent molecules

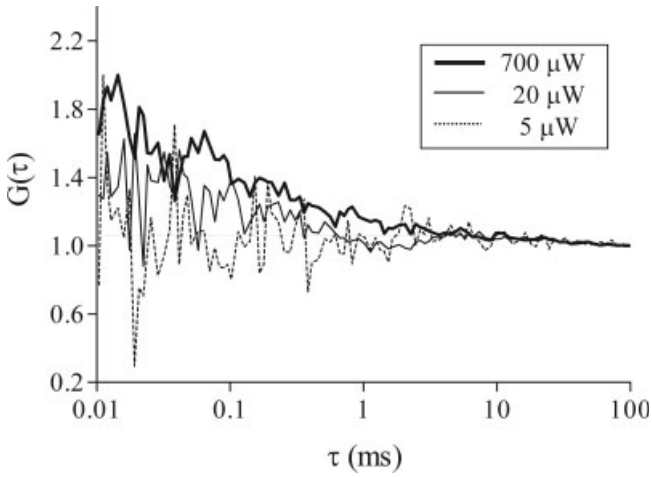

Fig. 6. Normalized autocorrelation curves from *Dictyostelium* autofluorescence at different excitation intensities at 488 nm. Data were acquired for 10 s from cells incubated in potassium phosphate buffer (pH 6.5, 17 mM).

TABLE 1. Autofluorescence intensities of Dictyostelium AX3 cells under different conditions

Condition	I (kHz)	No. of cells
HG5 Medium	85 ± 30	40
Buffer		
~15 min	44 ± 17	15
~1 h	37 ± 16	38
~4 h	41 ± 20	39
1–2 s photobleaching (1mW)	16 ± 7	20
5–7 s photobleaching (1mW)	8 ± 3	20

Average autofluorescence intensities and standard deviations were obtained from 10 s measurements. Cells, incubated in either HG5 medium or potassium phosphate buffer (pH 6.5, 17 mM), were excited with 488 nm argon-ion laser line with power of ~10 μW.

TABLE 2. PCH analysis of Dictyostelium autofluorescence

Condition	ε (kHz/molecule)	N	C (nM)	I (kHz)	No. of cells
No photobleaching	0.43 ± 0.3	89 ± 35	107 ± 42	33 ± 14	12
1–2 s photobleaching (1mW)	0.33 ± 0.1	42 ± 17	50 ± 20	13 ± 8	17

Average values and standard deviations for brightness (ϵ), number of molecules in confocal detection volume (N), calculated average concentration (C), and fluorescence intensity (I) were obtained for wild type AX3 cells incubated in potassium phosphate buffer (pH 6.5, 17mM), excited at 488 nm. The average concentration was calculated using Eq. (5). Photons (3×10^5–1×10^6) were acquired at excitation intensity of ~10 μW. Data were analyzed at a sampling frequency of 20 kHz.

throughout the cell can be photobleached and no recovery would be seen during a subsequent FFS measurement. The high laser intensity does not appear to harm the cells as they retain their irregular shape and continue to move. Thus, bleaching cells prior to FFS measurements on GFP fusion proteins can minimize the influence of autofluorescence.

The molecular brightness and concentration of autofluorescent molecules in cells incubated in buffer, with and without short photobleaching for 1–2 s, was quantified using PCH analysis (Table 2). As expected, prebleaching does not affect the average molecular brightness of the autofluorescent molecules, but the average concentration reduces by around 50%. Under similar experimental settings, the HG5 medium had a brightness value of 0.2 kHz, similar to what is observed in cells. But the concentration of the fluorescent species, of ~1 μM, is much higher than in cells. An eGFP solution in Tris buffer (pH 8) has ~7 times higher molecular brightness corresponding to a value of 2.57 ± 0.02 kHz. Since the relative contribution of different species to the autocorrelation curve is weighted by the square of the molecular brightness (Eqs. (1) and (2)), eGFP will contribute at least 50 times more to the autocorrelation curve, when the average number of eGFP molecules in the detection volume is equal to or higher than the autofluorescent molecules.

DISCUSSION

Autofluorescence from cells is a major factor leading to reduced SNRs and artifacts in fluorescence microscopy measurements in cells. In this study, the spectral properties of *Dictyostelium discoideum* autofluorescence have been characterized using fluorescence microscopy. Whole cell autofluorescence spectra obtained using spectral imaging microscopy show that *Dictyostelium* autofluorescence covers a wide wavelength range from ~500 to 650 nm. Cellular autofluorescence in this wavelength range has been attributed to biomolecules such as flavin nucleotides, flavoproteins, and NAD(P)H (Aubin, 1979; Benson et al., 1979). At the excitation wavelength (~435 nm) used in this study, NAD(P)H cannot be excited. Hence, the detected autofluorescence results from flavin compounds. The spectrum of free FMN obtained under similar experimental conditions overlaps with the autofluorescence spectrum to a large extent, but is slightly red-shifted. Also the spectrum of the growth medium HG5, which contains the vitamin riboflavin, shows nearly complete overlap with autofluorescence and FMN spectra. The differences in the spectra of HG5, free FMN, and autofluorescence can be attributed to the sensitivity of flavin fluorescence to its environment. Thus, factors such as pH, differences in viscosity and binding of FMN to proteins or peptides in both cells and the growth medium, would affect the spectrum (Aubin, 1979; Benson et al., 1979; Visser et al., 2001).

The autofluorescence covers the entire eGFP emission range and potentially interferes with fluorescence measurements of eGFP fusion proteins in cells. One way of minimizing interference of autofluorescence would be to fuse proteins of interest with other, more red-shifted fluorescent proteins, e.g., mRFP or dTomato (Fischer et al., 2004; Shaner et al., 2004). Another way would be to reduce the autofluorescence signal such that its influence on the measurements reduces. To find means of achieving the latter, the autofluorescence characteristics were further studied using fluorescence confocal microscopy and fluctuation spectroscopy. The autofluorescence intensity can be reduced by around 50% by incubating the cells in buffer instead of the growth medium. The reduction is rapid, in agreement with reported fluid uptake rates by axenically grown AX3 cells. The residual autofluorescence, after the exchange of the growth medium with buffer, does not change with time, suggesting that the remaining autofluorescent molecules are probably necessary for the cell functioning and cannot be exchanged by the cell. However, this intensity of the autofluorescent molecules can be further reduced by another 85% by photobleaching with high laser powers for short periods of time. As the high laser powers do not change the morphology and behavior of the cells and the autofluorescence reduces faster than the GFP fluorescence, prebleaching can be a convenient way of reducing autofluorescence interference. However, since bleaching would also reduce the signal from GFP, the time for which cells are exposed to high intensity should depend on the expression level of the GFP fusion proteins.

The extent of interference of autofluorescence in FFS depends on the concentration and molecular brightness of the autofluorescent molecules compared with those of GFP or other fluorophores being used. In PCH analysis, the presence of autofluorescence can be taken into account using a model for two fluorescent species, with one species fixed to the autofluorescence parameters (Chen et al., 2002). In autocorrelation curves, autofluorescence can either introduce a steady background of noncorrelating species or an additional correlating component. The *Dictyostelium* autofluorescence did not show autocorrelation at excitation intensities lower than 20 μW. The presence of noncorrelating background does not affect the diffusion times obtained from FCS curves, but can influence the amplitude of the autocorrelation curve, which should be corrected. At excitation intensities above 20 μW, the autofluorescence intensity fluctuations autocorrelate. However, the relatively high eGFP brightness, in cases where the average number of autofluorescent molecules in the detection volume is expected to be less than the average number of eGFP molecules, would make the

autofluorescence contribution to the autocorrelation curve negligible.

To summarize, *Dictyostelium* autofluorescence displays a wide spectrum with a peak at ~510 nm and potentially interferes with measurements of GFP fusion proteins with fluorescence microscopy techniques. The autofluorescence is localized in discrete areas in the cell and the localization pattern and intensity do not change with long incubations in buffer. For FFS measurements, the interference from autofluorescence can be minimized by incubating cells in buffer, prebleaching, and making use of low excitation intensities.

REFERENCES

Aguado-Velasco C, Bretscher MS. 1999. Circulation of the plasma membrane in *Dictyostelium*. Mol Biol Cell 10:4419–4427.

Aubin J. 1979. Autofluorescence of viable cultured mammalian cells. J Histochem Cytochem 27:36–43.

Benson R, Meyer R, Zaruba M, McKhann G. 1979. Cellular autofluorescence—is it due to flavins? J Histochem Cytochem 27:44–48.

Blaauw M, Knol JC, Kortholt A, Roelofs J, Ruchira , Postma M, Visser AJWG, Van Haastert PJM. 2003. Phosducin-like proteins in *Dictyostelium discoideum*: implications for the phosducin family of proteins. EMBO J 22:5047–5057.

Bretschneider T, Jonkman J, Kohler J, Medalia O, Barisic K, Weber I, Stelzer EH, Baumeister W, Gerisch G. 2002. Dynamic organization of the actin system in the motile cells of *Dictyostelium*. J Muscle Res Cell Motil 23:639–649.

Brock R, Hink MA, Jovin TM. 1998. Fluorescence correlation microscopy of cells in the presence of autofluorescence. Biophys J 75:2547–2557.

Brock R, Vamosi G, Vereb G, Jovin TM. 1999. Rapid characterization of green fluorescent protein fusion proteins on the molecular and cellular level by fluorescence correlation microscopy. Proc Natl Acad Sci USA 96:10123–10128.

Chen Y, Müller JD, So PT, Gratton E. 1999. The photon counting histogram in fluorescence fluctuation spectroscopy. Biophys J 77:553–567.

Chen Y, Müller JD, Ruan Q, Gratton E. 2002. Molecular brightness characterization of eGFP in vivo by fluorescence fluctuation spectroscopy. Biophys J 82:133–144.

Fischer M, Haase I, Simmeth E, Gerisch G, Muller-Taubenberger A. 2004. A brilliant monomeric red fluorescent protein to visualize cytoskeleton dynamics in *Dictyostelium*. FEBS Lett 577:227–232.

Haustein E, Schwille P. 2003. Ultrasensitive investigations of biological systems by fluorescence correlation spectroscopy. Methods 29:153–166.

Hess ST, Huang S, Heikal AA, Webb WW. 2002. Biological and chemical applications of fluorescence correlation spectroscopy: a review. Biochemistry 41:697–705.

Hink MA, Borst JW, Visser AJ. 2003. Fluorescence correlation spectroscopy of GFP fusion proteins in living plant cells. Methods Enzymol 361:93–112.

Janetopoulos C, Jin T, Devreotes PN. 2001. Receptor-mediated activation of heterotrimeric G-proteins in living cells. Science 291:2408–2411.

Jin T, Zhang N, Long Y, Parent CA, Devreotes PN. 2000. Localization of the G protein βγ complex in living cells during chemotaxis. Science 287:1034–1036.

Kayman S, Clarke M. 1983. Relationship between axenic growth of *Dictyostelium discoideum* strains and their track morphology on substrates coated with gold particles. J Cell Biol 97:1001–1010.

Kriebel PW, Barr VA, Parent CA. 2003. Adenylyl cyclase localization regulates streaming during chemotaxis. Cell 112:549–560.

Levin MK, Carson JH. 2004. Fluorescence correlation spectroscopy and quantitative cell biology. Differentiation 72:1–10.

Parent CA, Blacklock BJ, Froehlich WM, Murphy DB, Devreotes PN. 1998. G-protein signaling events are activated at the leading edge of chemotactic cells. Cell 95:81–91.

Potma EO, de Boeij WP, Bosgraaf L, Roelofs J, Van Haastert PJ, Wiersma DA. 2001. Reduced protein diffusion rate by cytoskeleton in vegetative and polarized *Dictyostelium* cells. Biophys J 81:2010–2019.

Ruchira , Hink MA, Bosgraaf L, Van Haastert PJM, Visser AJWG. 2004. Pleckstrin homology domain diffusion in *Dictyostelium* cytoplasm studied using fluorescence correlation spectroscopy. J Biol Chem 279:10013–10019.

Schwille P, Meyer-Almes FJ, Rigler R. 1997. Dual-color fluorescence cross-correlation spectroscopy for multicomponent diffusional analysis in solution. Biophys J 72:1878–1886.

Shaner NC, Campbell RE, Steinbach PA, Giepmans BNG, Palmer AE, Tsien RY. 2004. Improved monomeric red, orange and yellow fluorescent proteins derived from *Discosoma* sp. red fluorescent protein. Nat Biotechnol 22:1567–1572.

Skakun VV, Hink MA, Digris AV, Engel R, Novikov EG, Apanasovich VV, Visser AJ. 2005. Global analysis of fluorescence fluctuation data. Eur Biophys J 34:323–334.

Tsien RY. 1998. The green fluorescent protein. Annu Rev Biochem 67:509–544.

Uchida KSK, Yumura S. 2004. Dynamics of novel feet of *Dictyostelium* cells during migration. J Cell Sci 117:1443–1455.

Veltman DM, Roelofs J, Engel R, Visser AJWG, Van Haastert PJM. 2005. Activation of soluble guanylyl cyclase at the leading edge during *Dictyostelium* chemotaxis. Mol Biol Cell 16:976–983.

Visser AJWG, vdBerg PAW, Hink MA, Petushkov VN. 2001. Fluorescence correlation spectroscopy of flavins and flavoproteins. In: Rigler R, Elson ES, editors. Fluorescence correlation spectroscopy: theory and applications. Berlin: Springer-Verlag. pp 9–24.

Vukojevic V, Pramanik A, Yakovleva T, Rigler R, Terenius L, Bakalkin G. 2005. Study of molecular events in cells by fluorescence correlation spectroscopy. Cell Mol Life Sci 62:535–550.

Widengren J. 2001. Photophysical aspects of FCS measurements. In: Rigler R, Elson ES, editors. Fluorescence correlation spectroscopy: theory and applications. Berlin: Springer-Verlag. pp 276–301.

Xu X, Meier-Schellersheim M, Jiao X, Nelson LE, Jin T. 2005. Quantitative imaging of single live cells reveals spatiotemporal dynamics of multistep signaling events of chemoattractant gradient sensing in *Dictyostelium*. Mol Biol Cell 16:676–688.